Analysis of service failures of a cast iron mold in the glass packaging industry

Constança Maria Videira Correia
constanca.correia@tecnico.ulisboa.pt

Instituto Superior Técnico, Universidade de Lisboa, Portugal

October 2020

Abstract

This dissertation follows the identification of a ribbon tear defect (visual defect characterized by a superficial tear in the region of the body or neck of the glass piece) in the produced items and aimed to identify the origin of this failure. For this purpose, a comparative study of a blank mold from lot 06 (reference lot) and another from lot 07 was carried out, evaluating: the chemical composition, metallographic analysis, mechanical performance and thermal performance.

First, a thermographic analysis was carried out with the identification of 3 zones where the remaining tests were carried out. Then a chemical analysis was carried out, confirming a gray cast iron with a hypereutectic composition in both batches. Through an X-ray Diffraction analysis, the presence of the graphite and ferrite phases in the matrix was identified. This was followed by a metallographic analysis, where the microstructure of the graphite and the matrix was evaluated. This analysis was able to justify different heat flows between the molds and confirm the presence of ferrite as the predominant phase of the matrix, in addition to perlite and some carbides. Using the Scanning Electron Microscopy technique, a significant presence of molybdenum, manganese and vanadium carbides was revealed in both molds. The study was complemented with a hardness analysis, where we verified that the area in contact with the glass and the area behind the molds have different hardnesses, the highest values being in contact with the glass. Finally, the dilatometric analysis showed a minimal discrepancy in the coefficients of linear thermal expansion between the molds.

Keywords: Gray cast iron, blank molds, glass defect, and metallographic analysis.

1. Introduction

The company BA Glass was founded in 1912 by Raul da Silva Barbosa and Domingos de Almeida under the name Sociedade Barbosa & Almeida (automated production and commercialization of glass packaging). They started their business in 1930, in Campanhã-Porto, with the glass packaging factory Barbosa & Almeida Lda. The group expanded beyond national borders and now has an international presence (2001-Spain; 2012-Poland; 2016-Germany; 2017- Greece, Bulgaria and Romania). BA Glass is present in 7 countries with a total of 12 plants**. (BA Glass)**

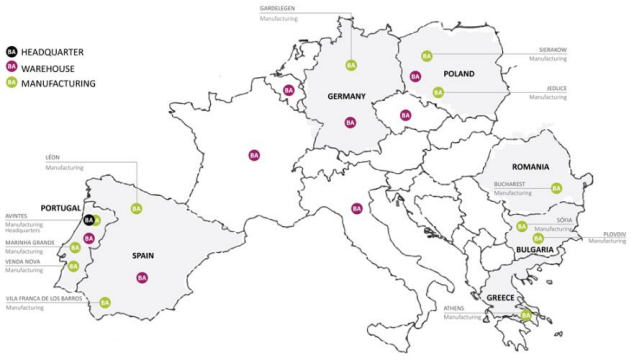

Figure 1- BA Glass plants.

2. State-of-the-Art

Automated process of the manufacture of container glass

The automated process of container glass (packaging glass in the present study) is divided into 6 distinct stages. The first, called glass composition, involves the formulation of the paste (glass and chemical composition) and the storage, dosage and mixing of raw materials that make up the batch to be placed in the furnace. Then comes (in the second phase) the batch fusion (in a regenerative furnace, under temperatures ranging between 1400°C and 1500°C), homogenization and refinement of the vitreous paste inside the furnace. The third phase involves the molding/shaping of glass, which in the automated manufacture of container glass takes place in the blow-and-blow process or the press-and-blow process. After the molding, (the fourth phase) the annealing and surface treatments provide the relief of mechanical tension present in the glass and allow for a surface finish. During quality control (in the fifth phase), the glass items are taken to automatic inspection machines to detect any possible defects (and elimination of items that do not conform to the client's contract documents). Lastly, (the sixth phase), the glass items are dispatched.

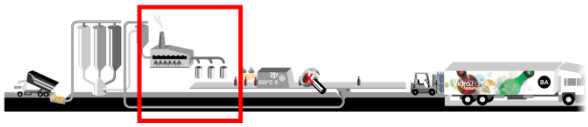

Figure 2-Automated process of the manufacture of container glass

Moulding of container glass

After the furnace comes the work tank (~1220°C). Here the vitreous paste is distributed through the distribution channels (*forehearths)* where it is thermally conditioned. **(Forming, 2002)** Throughout the distribution channels, several feeders are located. **(Le Bourhis, 2014)** The gobs of glass formed in the feeder feed the I.S. machines. Characteristics such as length, shape and drop weight (determinants for the success of the molding) are defined by the feeder. Once the gob is formed it falls vertically, by gravity, directly into the cavity of the I.S. machine through channels and deflectors. The automatic molding machines (IS machines) are made up of 10 to 12 sections that operate independently. Line 24 is made up of 10 independent sections. In each section the molding is processed in 2 stages: in the first (beginning stage) a model is made (or preliminary or parison) of the piece of glass and in the second stage (final stage) the final shape of the piece is formed.

In the press and blow process, the gob is placed into a blank mold through a funnel, which is immediately removed and replaced with a lid. Then the plunger begins it's vertical movement, pressing the glass against the lid. After covering it completely, the vitreous paste 'runs' down the walls of the blank mold as far as the nozzle, providing a rough shape of the finish of the glass packaging. The model (held by the finish part) is then transferred to the final mold, where the final shaping will take place. The final blow (in which compressed air is injected into the model) allows the definition of the final shape of the piece. After opening the mold, a clamp secures the piece at the finish part and places it on a ventilated mat, which facilitates cooling. **(Sarwar & Armitage, 2003)**

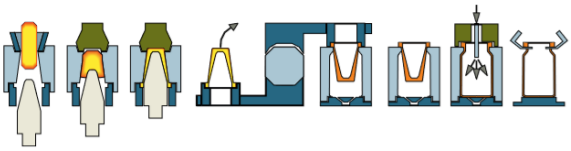

Figure 3-Press and blow process

Defects in glass

The automatic manufacture of glass (container and flat) has undergone significant technological advances and improvements in process over the years. These have significantly reduced the number and type of defects and non-conformities in the pieces. However, defects and/or non-conformities appear (albeit sporadically) that could compromise the manufacture and/or profitability of the process.

In this work, the defect under study is ribbon tears, and it involves molding defects. Ribbon tears are a visual defect characterized by a surface tear in the body or neck of the piece of glass, originating on the starting side (blank mold side).**("Glass container defects," n.d.)**

Table 1-Possible causes of the ribbon tears defect

Feeder	Machine setup and operation	Mold equipment
Glass too cold	Cold plunger	Dirty blank
	Excessive plunger pressure	Incorrect blank design
	Incorrect blank and blow mold	Interference between neck ring and blank

	linkage alignment	mold neck ring diameter too large
	Excessive cooling of blank mold	Blank and mold warped and/or worn out
	Insufficient blank mold dwell time.	Blank and molds insufficiently hollow scraped
	Interlock between blank and ring dirty, causing neck to open when blank opens	Blank molds of different matrices, with different mechanical and/or thermal performance

Blank molds

Blank molds are the metallic components used in the glass industry that allow, in the first phase of molding (starting side) the formation of a first version of the piece of glassware to be produced. For the success of this operation it is necessary that they possess a good surface finish at the point which is in contact with the glass. **(Mashloosh, 2015**) It is equally important that they can provide efficient heat transfer in order for a rapid cooling of the melted glass to take place (allowing for faster production times) as well as a good distribution of temperatures (avoiding mechanical distortions in the glass, namely asymmetries in the relaxation profile). **(MANNS, DÖLL, & KLEER, 1994)**

Figure 4-Blank mold 6802

Since high production speeds are demanded in the glass packaging industry, these molds are subject to short thermic cycles and great thermic amplitudes (they are in direct contact with the gob of glass, which falls into the mold cavity at a temperature of around 1050 °C). **(Cingi, Arisoy, Başman, & Şeşen, 2002)**

These operating conditions result in high mechanical tensions and related issues of fatigue, oxidation, corrosion, wear, fissuration and possible difficulties when unmolding. As a consequence, these components have been shown to fail prematurely (which implies frequent repair or even substitution). Currently the base materials most commonly used in the construction of molds for the glass industry are: cast iron, bronze-aluminium. These materials are cheap and perform well at high temperatures.

Cast iron

The term cast iron identifies a broad family of ferro-alloys with multiple components that solidify through an eutectic reaction. The iron, carbon and silicon are the major elements (referred to as alloying elements> 0.1%). They also present minor elements (<0.1%). (Figure 5) shows the binary balance diagram for the 2 major elements of the alloy -Fe-C. **(Stefanescu, 1990)**

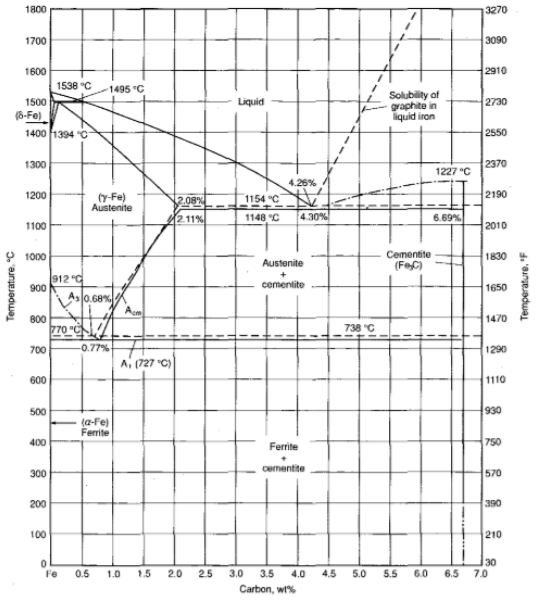

Figure 5-binary balance diagram for the 2 major elements of the alloy -Fe-C

Gray cast iron

The gray cast irons are chosen for use in diverse industrial applications since they display the following characteristics **(Pero-Sanz Elorz et al., 2018)**:

-Low cost: 20 to 40% less than steel;

-Good machinability, due to the presence of lamellar graphite in the metal mold, reducing the shear forces. The lamellar graphite also acts as a solid

lubricant during machining, reducing the need for lubricant;

-Reduced contraction during solidification (close to 1% of lineal contraction), due to the low density. The density of cast iron is between 6.95 gcm3 and 7.35 g/cm3, decreasing with the level of carbon (graphite displays a density of ~2.2 g/cm, and can occupy a volume between 6% to 7% of the total volume);

-Excellent vibration dampening capacity;

-Good resistance to mechanical wear;

With a view to obtaining these properties, the selection of the composition of the alloy must take into consideration the following three basic structural elements:

i) shape, size and distribution of the graphite desired;

ii) structure free of carbides, and

iii) matrix.

Alloying elements

In the gray cast irons metallic elements are added to the alloy Fe-C, in order to improve the thermic and/or mechanical properties according to the desired application. These new metallic elements influence the potential for graphitisation (i.e. the capacity of cast iron to form the graphite phase, the structure and the final properties of the mold.

The alloy elements that favour the formation of graphite are called graphitising elements. The graphitising elements have the capacity to dissolve the embryos of Fe and C (essential in the formation of cementite), which slows the formation of cementite and favours the precipitation of graphite.

The (thermodynamic) role of a third element in the solubility of the carbon in the system Fe-C-X (where X represents the third element) can be classified in the following way (Table 6):

i) Elements that enhance graphitisation (positive role)

ii) Elements that delay graphitisation (negative role)

iii) Neutral elements in graphitisation (neutral role).

3. Materials and Methods

Materials

Two metal gray cast iron blank molds, from article 6802, supplied by the metalworking company OMCO:

i) Batch 06 (blank mold reference)

ii) Batch 07 (blank mold in study)

Preparation of metallic samples
Transversal section

For each blank mold (batches 06 and 07) 3 transversal sections (each with a thickness of 20 mm) were prepared. The transversal sections were obtained by cutting (using a saw) followed by milling. Figure 6 shows the level of each transversal section and figure 7 the identification of the front and side areas of a section.

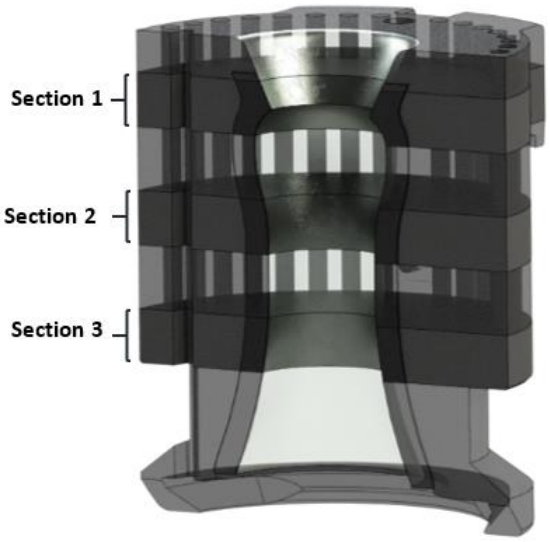

Figure 6-Level of each transversal section

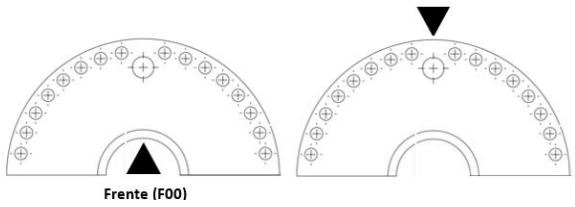

Figure 7-Identification of the front and side areas of a section.

Polishing of samples

Polishing was carried out manually in a Struers Rotopol-1 machine, using silicon carbide abrasive paper of successively decreasing grit (120, 220, 320, 600, 800, 1000, 2400 and 4000 m). The polishing time of each paper was 2 minutes, to enable the elimination of previous sanding scratches and to obtain a mirrored appearance.

RAM cloths were also used, with 6 µm e 1 µm diamond paste. Finally, to obtain an ultra fine polish, a colloidal silica suspension was used (OPS). As a way to enhance the polishing, and to allow the surfaces to remain flat, the samples were placed in phenolic resin, as illustrated in figure 8.

Chemical contrast of the samples

The chemical attack was carried out with Nital 2% (2 nitric acid and 96 of ethanol). Nital reveals the microstructure through the darkening of the perlite and highlighting of the ferrite grain seals. The chemical attack was 5 seconds.

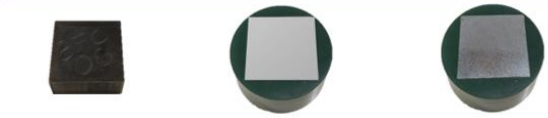

Figure 8-Sample preparation steps

Methods

The elementary quantitative chemical composition of the samples was performed by X-ray Fluorescence. The test was carried out on the WD-FRX Axiosmax 4 kW equipment with a Rhodium ampoule, using calibration lines obtained with 26 patterns of different types of cast iron. RBS measurements were made at the CTN/IST Van de Graaff accelerator. RBS measurements were made in the small chamber were three detectors are installed: standard at 140º, and two pin-diode detectors located symmetrical each other, both at 165º (detector 3 on same side as standard detector 2). Spectra were collected for 1.8 and 2 MeV $^{1}H^{+}$. Normal incidence was used in the experiments. PIXE experiments were also made. XRD characterization was performed with D8 Advance (Bruker) with Linxeye xE detector (tension of 40kV and current 40mA). A JEOL field emission scanning electron microscope (FE-SEM) model JSM-7001F equipped with an Oxford Light Elements EDS Detector and a HITACHI model S-2400 with a Bruker Esprit 1.9, EDS Bruker SDD light element detector were used. Hardness tests were performed in DuraVision equipment. The dilatometric analyzes were performed on the BÄHR-Thermoanalyse GmbH dilatometer, type DIL 801L, in the temperature range 25°C to 934.9°C, test atmosphere: air and horizontal measurement system: alumina (up to 1600°C in air).

4. Experimental Results and Discussion

Chemical composition

Table 2-Chemical composition analysis

	BA Glass	XRF		RBS e PIXE	
Elements (weight %)	**Lotes 06 e 07**	**Lote 06**	**Lote 07**	**Lote 06**	**Lote 07**
Fe	Base 92,927	Base (95,969-C)	Base (96,371-C)	90,515	90,469
C	3,57 ± 0,08	*	*	4,841± 0,121	4,889±0,122
Si	2,00 ± 0,10	2,226 ± 0,223	2,309 ± 0,231	3,156±0,079	3,155±0,079
Mn	0,60 ± 0,10	0,631 ± 0,063	0,536 ± 0,054	0,579±0,014	0,579±0,014
Mo	0,53 ± 0,08	0,548 ± 0,055	0,439 ± 0,044	0,505±0,013	0,505±0,013
Cu	0,00 ± 0,50	0,212 ± 0,021	0,064 ± 0,006	-	-
Ti	0,22 ± 0,03	0,164 ± 0,016	0,172 ± 0,017	0,168±0,004	0,168±0,004
Ni	0,00 ± 0,50	0,136 ± 0,014	0,045 ± 0,005	-	-
Cr	0,00 ± 0,20	0,114 ± 0,011	0,064 ± 0,006	0,091± 0,002	0,091± 0,002
V	0,12 ± 0,03	0,108 ± 0,011	0,083 ± 0,008	0,089±0,002	0,089±0,002
S	0,033 ± 0,027	0,052 ± 0,005	0,035 ± 0,0035	-	-
P	0,00 ± 0,20	0,050 ± 0,005	0,051 ± 0,005	0,054±0,001	0,054± 0,001
Zn	-	0,041 ± 0,004	0,002 ± 0,0002	-	-
Al	-	0,016 ± 0,002	0,013 ± 0,001	-	-
Mg	-	0,011 ± 0,001	0,001 ± 0,0001	-	-
Co	-	0,009± 0,0009	0,001 ± 0,0001	-	-
Sn	-	0,005 ± 0,0005	0,005 ± 0,0005	-	-
Nb	-	0,005 ± 0,0005	0,005 ± 0,0005	-	-
Sb	-	0,003 ± 0,0003	0,003 ± 0,0003	-	-
As	-	0,002 ± 0,0002	0,002 ± 0,0002	-	-
Zr	-	0,002 ± 0,0002	0,002 ± 0,0002	-	-
Pb	-	0,001 ± 0,0001	0,001 ± 0,0001	-	-

According to the chemical composition (supplied and made), the metal alloy used for the manufacture of blank molds 06 and 07 is a gray cast iron.

By using formula 1 and 2 it was possible to determine the equivalent carbon value of the alloys.

$$CE = \%C + \frac{\%Si}{3} + \frac{\%P}{3} \quad \text{[Equation 1]}$$

$$CE = \%C + 0{,}3\ \%Si + 0{,}33\ \%P - 0{,}027\ \%Mn + 0{,}4\ \%S \quad \text{[Equation2]}$$

The equivalent carbon values are shown in table 3.

Table 3-Equivalent carbon values

	BA Glass		RBS e PIXE	
	06	07	06	07
Equation 1	4,24	4,24	5,91	5,96
Equation 2	4,17	4,17	5,79	5,84

According to the result obtained by the carbon equivalent formula, what is required by BA Glass would be a cast iron with a hypoeutectic composition, that is, an equivalent carbon value under 4.3%. Certificates from the OMCO confirm the presence of this type of composition, however according to the analyzed (RBS and PIXE), both lots show a hypereutectic composition, that is, an equivalent carbon value greater than 4.3%. Analyzing the effect of the carbon equivalent in the mechanical properties, in particular in the tensile strength, it is verified that when the first one increases, there is a decrease in the values of the second.

X-ray diffraction

The analysis of the diffractograms showed the presence of the ferrite phase (α-Fe) through the presence of its 5 peaks of maximum intensity, located in decreasing order of intensity in the following positions in 2 θ: 44.673°; 82,333°; 65,021°; 116.38° and 98.945°. Since the scan was carried out between 20° and 130°, the lowest peak of ferrite intensity is not present, which would be located at 137.13°. The presence of a peak at a position in 2 θ of 26.381°, corresponding to the peak of maximum intensity of the graphite, allowed to conclude the existence of this phase.

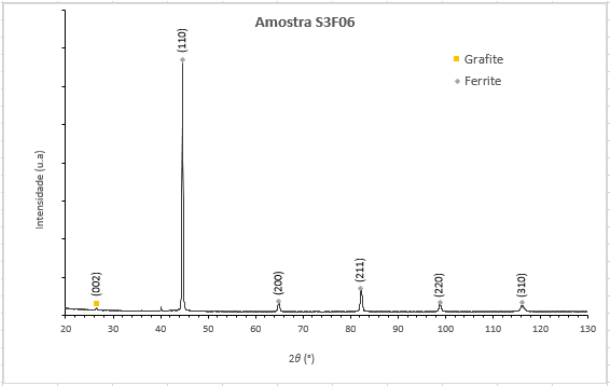

Figure 9-Diffractogram sample S3F06

Metallographic analysis

Table 4-Graphite analysis batch 06 (front)

Sample	Type, Distribution and size of the graphite	Fraction of the graphite (%)
S1F06	VII D8	~10
S2F06	VII D7	~15
S3F06	VII D7	~20

Table 5-Graphite analysis batch 07 (front)

Sample	Type, Distribution and size of the graphite	Fraction of the graphite (%)
S1F07	VII D7	~29
S2F07	VII D7	~27
S3F07	VII D7	~23

Table 6- Graphite analysis batch 06 (back)

Sample	Type, Distribution and size of the graphite	Fraction of the graphite (%)
S2T06	~ 70% VII A3, 30% VII D7	~18
S3T06	~ 50% VII A3, 50% VII D7	~19

Table 7- Graphite analysis batch 07 (back)

Sample	Type, Distribution and size of the graphite	Fraction of the graphite (%)
S2T07	~12% VII A5, 88% VII D7	~19
S3T07	~12% VII A6, 88% VII D8	~13

The metallographic analysis of samples 06 and 07 shows a significant difference. While in mold 06, front, the graphite content grows (to double) as it descends along the mold profile (from S1 to S2 and S3), mold 07 (front) the graphite content decreases (S1 > S2 > S3). This metallographic profile can contribute to a distinct flow of heat between the 2 molds.

With regard to lot 06, it was found that the samples: S1F06, S2F06 and S3F06, corresponding to the mold area in contact with the glass, present graphite with a randomly oriented interdendritic lamellar aspect corresponding to type VII and distribution D. Regarding the size of the present lamellae, it was observed that S1F06 falls in class 8 (graphite lamellas with dimension <10 µm) and the rest, S2F06 and S3F06, in class 7 (graphite lamellas with dimensions between 10 to <20 µm). Analyzing the present graphite fraction, it appears that S1F06 presents ~ 10%, S2F06 ~ 15% and S3F06 ~ 20%.

Regarding the area behind the mold (lot 06), it was observed that both samples: S2T06 and S3T06 exhibit graphite with a lamellar aspect corresponding to type VII, distributed in the matrix in two different ways: A (randomly oriented and evenly distributed) and D (randomly oriented interdendritic). They differ in the proportion of these distributions, with sample S2T06 showing ~ 70% graphite with A distribution and 30% graphite with D distribution and sample S3T06 showing ~ 50% graphite with A distribution and 50% graphite with D distribution. In both samples associated with distribution A, there is a class 3 lamellar dimension (graphite lamellas with dimensions between 160 to <320 µm) and associated with distribution D there is a class 7 lamellar dimension. The graphite fraction present in sample S2T06 is ~ 18% and in the S3T06 sample it is ~ 19%.

Regarding lot 07, it was observed that the front zone (S1F07, S2F07 and S3F07) has the same graphite type, distribution, and size as lot 06, with the exception of S1F07 which has a lamellar size greater than that observed in S1F06. It appears that the fraction of graphite present (S1F07 ~ 29%, S2F07 ~ 27% and S3F07 ~ 23%) is higher than that of batch 06.

The rear area (lot 07) shows the same graphite type and distribution as seen in lot 06. They differ in the proportion of this distribution as well as in the size of the lamellae, with a higher % of type D graphite in lot 07 associated with a smaller size (S2T07 ~ 12% of graphite with A distribution and size corresponding to class 5 and ~ 88% of graphite with D distribution and size corresponding to class 7; S3T07 ~ 12% of graphite with A distribution and size corresponding to class 6 (graphite lamellae with a dimension between 20 to <40 µm) and ~ 88% of graphite with D distribution and size corresponding to class 8). The graphite fraction present is identical to that of lot 06, with a slight decrease in S3T07 (S2T07 ~ 19% and S3T07 ~ 13%).

The microstructure of the graphite shown in both molds is in accordance with the requirements in the specifications dossier of BA Glass, with the exception of the lamellar size shown on the back of the molds, which is lower in the case of batch 07.

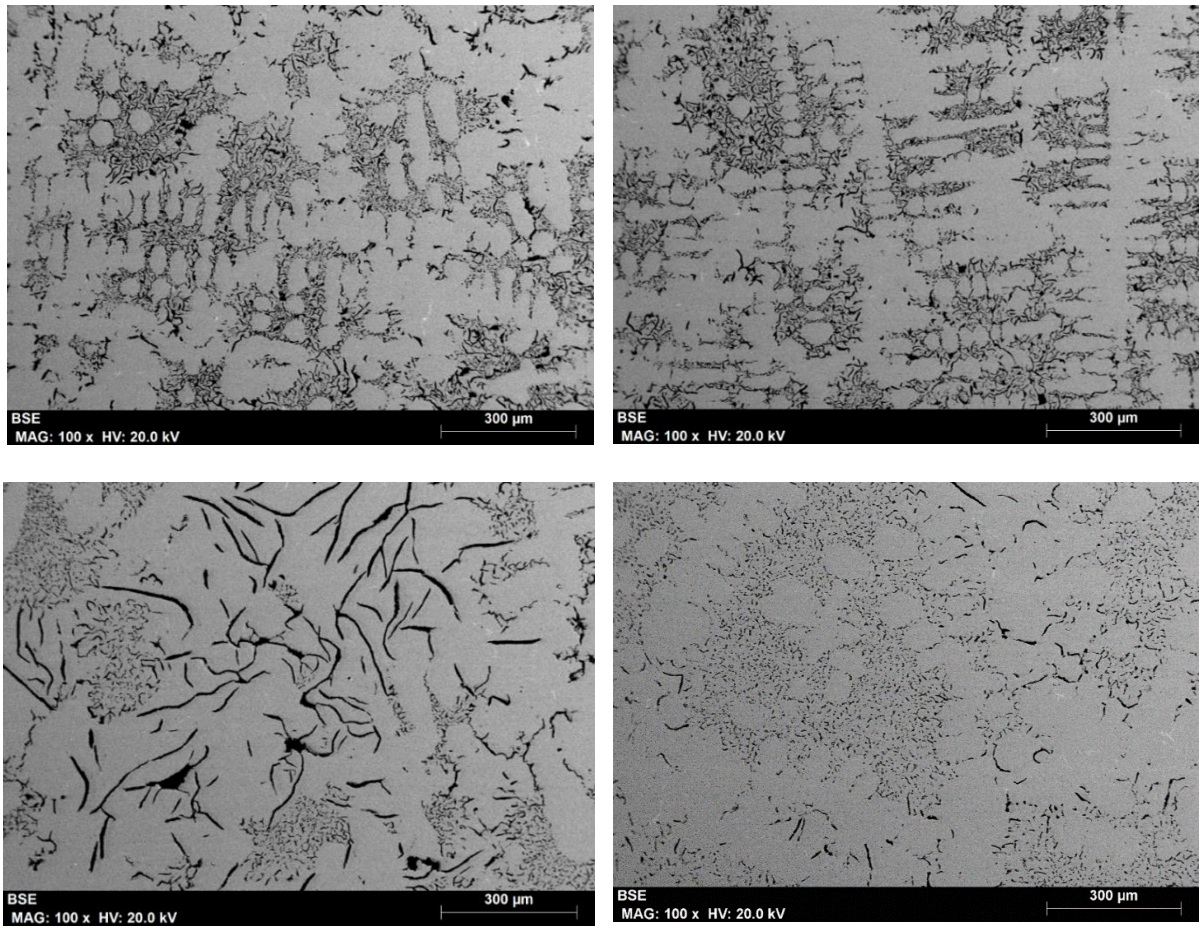

Figure 2-Samples S3F06, S3F07, S3T06 and S3T07

Hardness analysis

The analysis of the hardness values allowed to verify that in both molds the areas in contact with the glass (S1F06, S2F06, S3F06, S1F07, S2F07, S3F07) are the ones that present higher hardness values, as required by the company BA Glass, since they are the areas of the molds that present a more refined microstructure. In the case of lot 06, the average value for S1F06 was 149.50 HBW, for S2F06 it was 147 HBW, and for S3F06 145.17 HBW, with no great difference in values between the sections. With regard to lot 07, it was observed that the average value for S1F07 was 141HBW, for S2F07 it was 143.50 HBW and for S3F07 it was 141.17 HBW, which are also similar values. There is a decrease in the hardness values of the front sections of lot 07 in relation to those of lot 06.

The hardness values shown in the casting company certificates referring to the area under analysis are 156 HBW for lot 06 and 151 HBW for lot 07. These values are within what is required in the specifications dossier of 165 ± 15 HBW. However, they differ from the measured values, the latter being lower, and not within the specified limit. The discrepancies between the hardness values may be related to the fact that, both in the specifications dossier and in the certificates, there a single hardness value that they consider representative of this region of the mold, whereas in this analysis there were considered two regions in the mold with different dimensions, and the measurement zone may not coincide. This decrease in hardness compared to the established values, may result in finishing defects to the surface of the glass. With regard to the backs of the molds, there is a greater disparity between the hardness values, associated with the non-uniformity of the microstructure in this area of the mold. In the case of lot 06, the average value for S2T06 was 125.17 HBW, and for S3T06 it was 125.17 HBW. Regarding lot 07, the average value for S2T07 was 122.50 HBW and for S3TC06 it was 138.50 HBW. This last hardness value is associated with the refinement of the microstructure observed in this zone.

Table 6-Hardness values batch 06

	Hardness (HBW)						
	Measurements						
Sample	1	2	3	4	5	6	Average
S1F06	151	149	149	150	151	148	149,50 ± 1,21
S2F06	150	147	148	146	146	145	147,00 ± 1,79
S2T06	133	120	125	127	124	122	125,17 ± 4,54
S3F06	141	147	143	146	148	146	145,17 ± 2,64
S3T06	125	115	125	118	138	130	125,17 ± 8,28

Table 7-Hardness values batch 07

	Hardness (HBW)						
	Measurements						
Sample	1	2	3	4	5	6	Average
S1F07	141	141	142	140	141	141	141,00 ± 0,63
S2F07	146	144	145	144	142	140	143,50 ± 2,17
S2T07	124	115	114	125	122	135	122,50 ± 7,66
S3F07	140	141	140	142	142	142	141,17 ± 0,98
S3T07	137	140	138	136	141	139	138,50 ± 1,87

5. Conclusions

From the different analysis carried out, we concluded that thermographically the molds can be divided into 3 zones. Chemically, the composition of the 2 molds is a gray cast iron with a hypereutectic composition. In the X-Ray Diffraction analysis, no difference between the molds was identified. In the metallographic analysis, there was an opposition between the molds, with mold 06, in the front area, growing in graphite content as it descended along the profile of the mold (from S1 to S2 and S3), whereas mold 07 (front) decreased in graphite content (S1 > S2 > S3), which justifies different heat flows between the molds. The presence of ferrite was confirmed as the predominant phase of the matrix, with perlite and some carbides also present. With the Scanning Electron Microscopy technique, a significant presence of molybdenum, manganese and vanadium carbides was revealed in both molds, and also titanium in mold 07. The hardness values confirm the presence of a more refined microstructure in the front area (the one in contact with the glass) through higher values. In the area behind the molds, there was a greater disparity between the hardness values, being associated with the non-uniformity of the microstructure in this area. From the dilatometric analysis it was concluded that lot 06 has a coefficient of linear thermal expansion slightly higher than lot 07.

This set of data did not allow to explain the glitch defect, and the possibility that the fault has another origin, namely mechanical or thermal, is left open.

6. References

"BA Glass." [Online]. Available: http://www.bavidro.com/pt/.

Cingi, M., Arisoy, F., Başman, G., & Şeşen, K. (2002). The effects of metallurgical structures of different alloyed glass mold cast irons on the mold performance. *Materials Letters*, *55*(6), 360–363. https://doi.org/10.1016/S0167-577X(02)00393-2

Forming, G. (2002). Forehearths of the future. *Glass International*, *25*(3), 13.

Glass container defects. (n.d.).

Le Bourhis, E. (2014). *Glass: Mechanics and Technology: Second Edition*. *Glass: Mechanics and Technology: Second Edition* (Vol. 9783527337). https://doi.org/10.1002/9783527679461

MANNS, P., DÖLL, W., & KLEER, G. (1994). Glass in contact with mould materials for container production. *Glass Science and Technology (Frankfurt)*, *68*(12), 389–399.

Mashloosh, K. M. (2015). Wear resistance of different types of cast iron used in glass blow mould. *Diyala Journal of Engineering Sciences*, *08*(03), 1–21.

Pero-Sanz Elorz, J. A., Fernández González, D., & Verdeja, L. F. (2018). *Physical Metallurgy of Cast Irons*. *Physical Metallurgy of Cast Irons*. https://doi.org/10.1007/978-3-319-97313-5

Sarwar, M., & Armitage, A. W. (2003). Tooling requirements for glass container production for the narrow neck press and blow process. *Journal of Materials Processing Technology*, *139*(1–3 SPEC), 160–163. https://doi.org/10.1016/S0924-0136(03)00214-0

Stefanescu, D. M. (1990). ASM Handbook, Volume 1: Properties and Selection: Irons, Steels, and High-Performance Alloys: Compacted Graphite Iron. *Metals Handbook*, *1*(January 1990), 56–70. https://doi.org/10.1361/asmhba0001